

3.3 Experiment Description

To better understand the relationship between inertia and small-signal stability, I run a set of numerical simulations where I perturb different network locations at different inertia values. I use the set of generator locations as the test set of network locations (*i.e.* the green nodes in Figure [blah]). At each network location, I simulate a perturbation to the generator's power over a range of inertia values (0.01 – 20.0 with a step of 0.01). The range of inertia values includes all of the assigned values associated with the power system test case (see Section 3.1). To help with clarity, I call the generator that is being perturbed under different inertia values the VRG, and I refer to all other generators in the network as SGs. Finally, let a **scenario** refer to the set of experiments associated with a VRG network location. Thus, there are 90 scenarios associated with the 500 node network (90 locations \times 2000 inertia values = 180,000 total simulations), and 49 scenarios associated with the 200 node network (98,000 total simulations).

For each simulation I measure the response of each component using the energies defined in Equation 2.2. Specifically, I compute the root-mean square (RMS) of all the individual energies that contribute to the total system energy: the kinetic energies $\langle T_g \rangle$, the nodal potential energies $\langle V_i \rangle$, and the line potential energies $\langle U_\ell \rangle$. Recall from Section 2.1.1 that the kinetic energy is a function of the generator frequency and inertia constant; the nodal potential energy is a function of the power and angular positions of the loads and generators; and the line potential energy is a function of the connection strength and angular difference of the connected nodes. Additionally, as will be explained further in the next chapter, I also measure the RMS of the total energy associated with subgraphs of the network. In other words, for some subgraph S , I measure the RMS of $E_S = \sum_{g \in S} T_g + \sum_{i \in S} V_i + \sum_{\ell \in S} U_\ell$.¹

It is beneficial to describe the characteristics of these energies for one scenario before moving into a detailed analysis for all scenarios. Figures 3.1–3.3 plot these energies as a function of the VRG inertia value for one scenario. I have grouped the energies by their associated components. For

¹ This is, of course, *not* the same as $\sum_{g \in S} \langle T_g \rangle + \sum_{i \in S} \langle V_i \rangle + \sum_{\ell \in S} \langle U_\ell \rangle$.

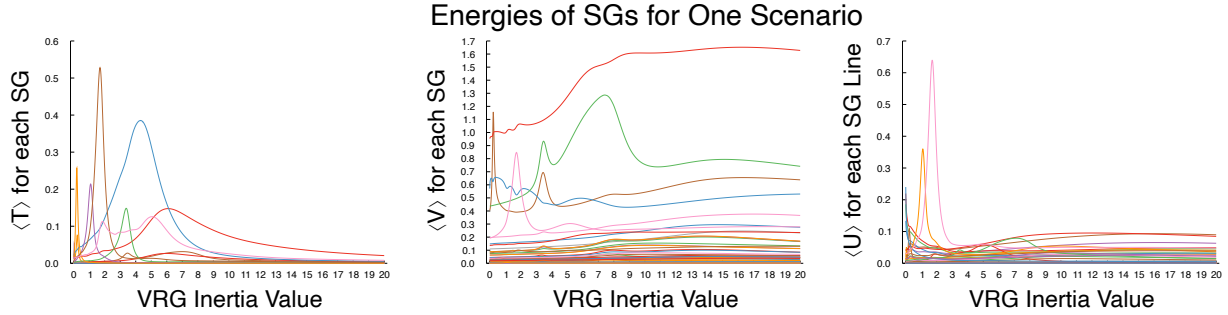


Figure 3.1: Example results for a single scenario where each value is plotted as a function of the VRG inertia constant. Each colored trace indicates the response of a generator where the colors are consistent across the plots (*i.e.* the pink curve refers to the same generator in each plot).

example, generators have kinetic energy, nodal potential energy, and a line potential energy. Due to the fact that both generators and loads are pendant nodes², they both have one line potential energy that can be associated with them.

Figure 3.1 plots the energies associated with the SGs of the example scenario. Each colored trace is associated with a different SG, and each SG has the same color in each plot.³ For each energy type there are distinct peaks in a few of the traces. For example, consider the blue trace in the far right plot of Figure 3.1. The peaks indicate that there is a particular VRG inertia value that causes an SG to fluctuate more than at other VRG inertia values. However, these peaks vary across SGs and across energy types. For example, the pink curves in the three plots of Figure 3.1 have a peak at approximately the same inertia value, but the shape of the pink curves are very different. The line potential energy has a very small width, while the kinetic energy has a very large width. Furthermore, the nodal potential energy has a larger height than the line potential and kinetic energy. These are some of the characteristics that are important for identifying the dynamical behavior of SGs.

Figure 3.2 plots the load energies as a function of the VRG inertia value. Similar to Figure 3.1, the colors of each trace in Figure 3.2 indicate separate loads, and a load has the same color

² They have a degree of one.

³ For example, the pink trace in all three plots refers to the same SG or, in the case of the line potential energy, the line that connects the SG to the network.

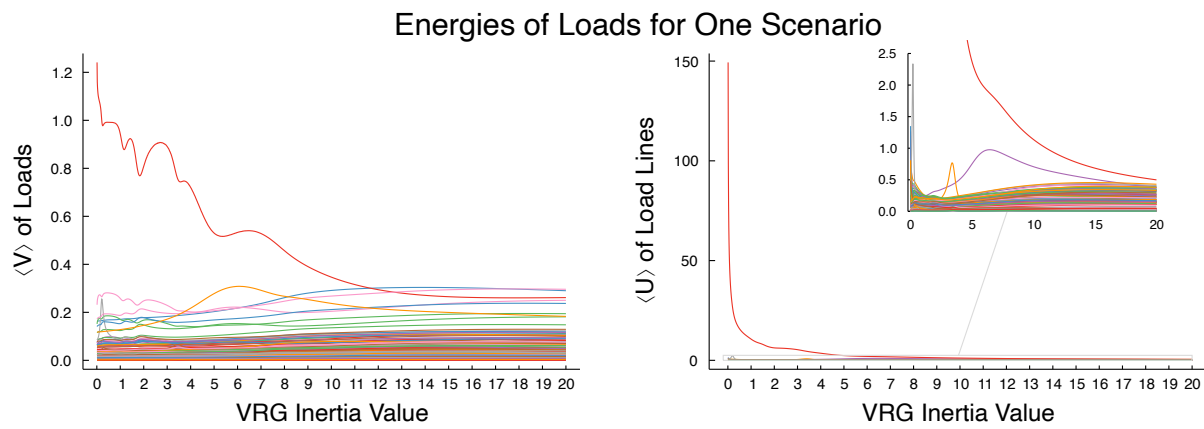


Figure 3.2: Example results for load nodes for the same scenario as Figure 3.1. Each colored curve indicates a different load node, with consistent coloring across the plots (*i.e.* the red curves refer to the same load node).

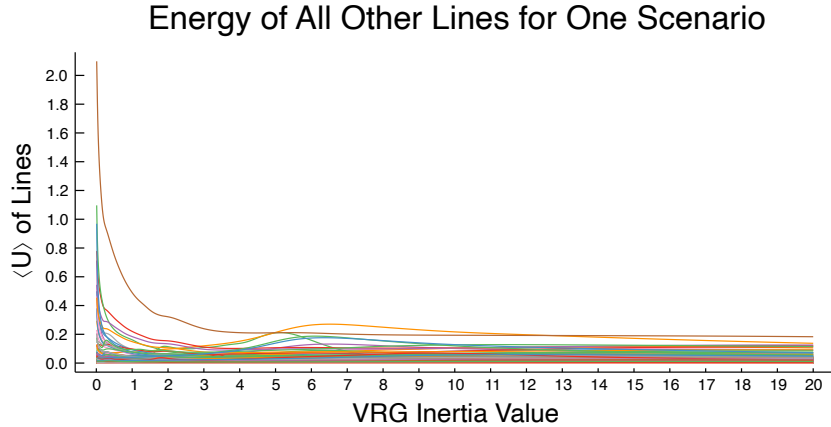


Figure 3.3: Example results of the potential energies for the lines that are not associated with generators or loads. Each colored trace indicates a separate line.

trace in each plot. Load nodes have an associated nodal potential energy and line potential energy. Although many of the curves in Figure 3.2 have peaks, the characteristics of the peaks are fairly different than those in Figure 3.1. For example, the red node potential energy curve in the left plot of Figure 3.2 has a unique shape: it decays (non-monotonically) with the VRG inertia value. The noticeable hills in this curve occur due to a similar phenomenon as the isolated peaks, but this load node does not have one isolated peak but many isolated peaks. The decaying of the red nodal potential energy and line potential energy indicates that this load node is very sensitive to the VRG inertia value across a large range rather than being sensitive at only a small range of VRG inertia values like most of the SG kinetic energy curves.

Finally, for completeness, Figure 3.3 plots the line potential energy of all lines that are not associated with a generator or a load. Again, each colored line corresponds to a different line in the network. There appear to be more or less two categories that these lines can be placed: those that decrease monotonically with the VRG inertia value and those that have a peak. The peaks of these line potential are wide and small in amplitude (as compared to the line potential energy peaks of the loads and generators).

Only a few curves in Figures 3.1|3.3 are distinct; for curves in the same energy type, many

have a similar shape with varying heights. For example, the inset of the right plot of Figure 3.2 shows many load lines with a similar shape but different amplitudes (in the range of 0.0 – 0.5). The similarity in the shape of the curves indicates that the fluctuations of those components are similar in frequency but are different in amplitude. The distinct curves, on the other hand, suggest dynamical behavior that is unique to that component. The next chapter analyzes these curves for all scenarios, specifically it characterizes the peaks: the inertia value where the peak occurs, the height, and the width. Each of these peak characteristics is a property of the node parameters (such as the inertia and damping constants) as well as the network structure. The next chapter explains why these peaks occur and what they mean for small-signal stability.

Chapter 4

Results

Recall from Section 2.1.3 that small-signal frequency stability is a category of power system oscillatory behavior that occurs due to small fluctuations in power consumption or generation. There are two types of oscillations that small-signal stability tends to address: local plant oscillations, and inter-area oscillations. Local plant oscillations consist of a few generators oscillating (in/out) of phase with each other, while the rest of the generators in the network oscillate together. Inter-area oscillations consist of one group of generators in one area of the system oscillating out of phase with another group of generators in a different area of the system.¹ In general, power system operators want to avoid both types of oscillatory behaviors. Historically, local plant oscillations occur the most frequently, and thus most generating plants make use of power system stabilizers to largely deal with this type of oscillation [citation]. On the other hand, inter-area oscillations can be harder to stabilize for a number of reasons: the number of units participating in the oscillation is often larger than that of local oscillations [citations]; the possibly large geographic spread of the participating generators can make it difficult to coordinate a stabilizing response [citations]; and, at times, the source of the oscillations can be challenging to determine [citations]. Thus, it is crucial to understand the impact of various system parameters and topologies on both types of oscillatory behaviors.

This thesis focuses on the impact of the inertia value at a specific network location on the small-signal stability of the rest of a power system. In particular, I show that small-signal stability

¹ Each group of generators is not necessarily entirely synchronized. This will be discussed further later in the chapter.

benefits from smaller inertia values; this is contrary to large-signal stability which benefits from larger inertia values. I demonstrate that there exists a range of VRG inertia values that elicit desirable small-signal stability properties across the network. Furthermore, I show that this range of VRG inertia values can be determined by the transition from local plant oscillations to inter-area oscillations. I determine that this transition from local to inter-area oscillations is highly dependent on the network location of the VRG *and* the local network structure that surrounds it. Thus, these results suggest that the network location of a VRG constrains the amount of inertial support that it can provide. This information can be used to help narrow a possibly large search space of placement and sizing of VRG inertial support.

To begin, I show how to identify local and inter-area oscillations from the system energies, which then allows me to identify the transition from local to inter-area oscillations. Recall from Section 3.3 that the term *scenario* indicates the set of experiments conducted by delivering a perturbation to a single network location, varying the inertia value at that location, and examining the response at all other nodes and links in the network (see Section 3.3 for further experimental details). Additionally, the term “VRG” refers to the perturbed generator with changing inertia constant for a given scenario. Finally, Sections 4.1 - 4.3 present results for the pulse perturbation type. Section [blah] compares these results for the stochastic perturbation type.

4.1 Identification of Local Oscillations

Localized oscillatory behavior can be identified using the RMS of the system energies after a perturbation is delivered. Recall from Section 3.3 that many of the energy response curves have well-defined peaks, as shown in Figure 4.1 (repeated here for reference). I characterize the peaks of these curves and then use this information to define the localized oscillatory response. The rest of this Section characterizes the peaks, specifically those related to the kinetic and nodal potential energies, for all scenarios. For now, I do not analyze the line potential energies because the peaks of the lines associated with generators and loads coincide with those for the nodal potential energy. For each peak, I analyze its VRG inertia value, height, and width.

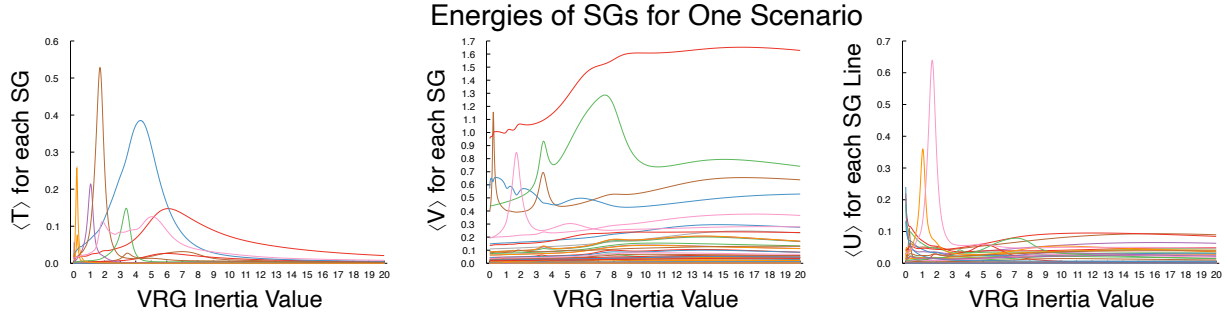


Figure 4.1: Example results for generators. Further details are provided in Section 3.3.

For every scenario, the inertia value that maximizes an SG or load response to the VRG perturbation is determined by the natural frequencies of the components involved in the behavior. Consider two generators with an electrical distance of F_{ij} (see Section 2.1.2). The natural frequency of generator i as seen by generator j is defined as $\sqrt{\frac{F_{ij}}{M_i}}$ [citation]. Thus, two generators where $F_{ij} \neq F_{ik}$ will “perceive” the natural frequency of generator i to be different for the same inertia value, M_i . Figure 4.2 plots the peak response for the kinetic (left) and nodal potential (right) as a function of the ratio of the VRG natural frequency to the SG or load natural frequency. In general, the closer the ratio is to one the more perturbation energy is absorbed by the component. This indicates that the energy exchange between the VRG and the SG/load is maximized when the frequencies match. As a consequence, the oscillations will take longer to decay for these components.

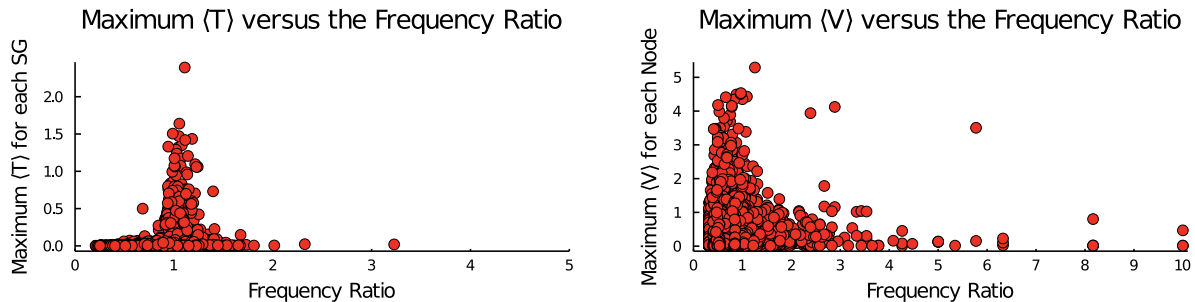


Figure 4.2: *Left:* Maximum kinetic energy response of an SG as a function of the ratio of the natural frequency of the SG and the VRG for each scenario. *Right:* Maximum potential energy response of a node as a function of the natural frequency ratio for each scenario.

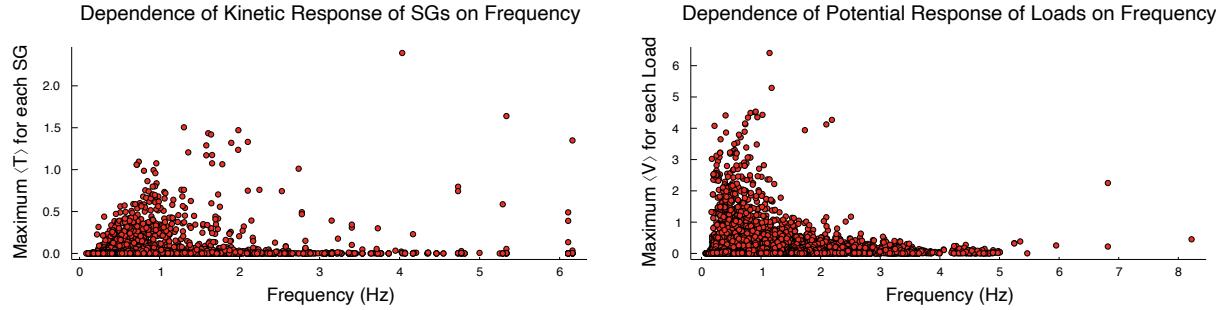


Figure 4.3: Each point corresponds to a peak value and all peaks for every scenario are plotted. *Left:* Maximum kinetic energy response of each SG as a function of the VRG frequency. *Right:* Maximum nodal potential energy of the SGs and loads as a function of the VRG frequency for each scenario.

The dependence of the energy absorption on the natural frequencies is a resonance phenomenon [citation]. Most oscillatory systems can have resonance phenomena, and this is not a new occurrence for power systems [citations]. Although local plant oscillations are not specifically defined by resonance, in this work I use the occurrence of resonance (*i.e.* the peaks) as the indicator of a local oscillation. Therefore, if a response curve does not have a peak (for example, the curves in Figure 3.3), I do not consider these components to have a localized response.

Not all local plant oscillations are equivalent, as is clear from the variation in the heights of the peaks in Figure 4.1. I conjecture that these variations depend on the VRG location and inertia value. Specifically, the peak heights vary according to the frequency of the VRG. Figure 4.3 plots the maximum energy absorption of generators and loads versus the frequency where that maximum occurs. Each point corresponds to one peak in one scenario, and all peaks from all scenarios are plotted. As the frequency becomes smaller (*i.e.* the inertia becomes larger), the kinetic and nodal potential energy absorption becomes larger. The frequencies of the nodal potential energy absorption tend to be smaller than the frequencies of maximal kinetic energy absorption. This indicates that at smaller inertia values, the perturbation energy is mostly absorbed in the form of kinetic energy (*i.e.* by generators), and at larger inertia values the perturbation energy is mostly absorbed in the form of nodal potential energy (*i.e.* by loads and generators). Additionally, the

maximal value of the nodal potential energies tend to be higher than that of the kinetic energies. This provides further evidence of the importance that load nodes play in small-signal stability [citations]. Specifically, at higher inertia values SGs can no longer help absorb the perturbation energy in the form of kinetic energy, and the nodal potential energy absorbs the majority of the perturbation energy.

[How to fit below paragraphs in? Not really the paragraphs I want to end the section on, but I think I need the previous paragraph about the relationship between the frequency and amplitude of the peak to define the full-width at half-max. Also not sure how it fits in with the rest of the work, but it is a characteristic of the peaks so I thought I should include it.]

The last important characteristic of the peaks are the widths: this is the damping ratio of the oscillation. The damping ratio of an oscillation indicates how quickly the oscillations will decay [citation]. In general, power system operators want oscillations to decay as quickly as possible under the limitations of the protective equipment [citation].

I determine the damping ratio of each peak by finding the full-width at half-max. In other words, I determine the two inertia values (one that is greater and one that is less than the peak inertia value) where the curve is equal to half of the maximum value. Let the difference between these two inertia values be β . I quantify the damping behavior of a local oscillation by the *quality factor* (Q factor) which is defined as the natural frequency divided by β . A higher Q factor indicates more damped oscillations, and a lower Q factor indicates less damped oscillations. Figure 4.4 plots the Q factor of each peak as a function of the natural frequency for the kinetic (left) and nodal potential (right) energies. The kinetic peaks with the highest Q factors occur within a frequency range of about 0.5 – 1.0 Hz. The nodal potential peaks with the highest Q factors occur within a frequency range of about 1 – 2 Hz. For peaks with lower frequencies, approximately 0 – 0.5 Hz, the Q factor decreases significantly. This occurs because the smaller the inertia value (the higher the frequency) is the less force is required to damp the oscillatory motion. Thus the peaks with higher inertia values (smaller frequencies) require more time to decay than those at smaller inertia values. Often any damping issues for specific oscillations are addressed via a Power System Stabilizer (PSS)

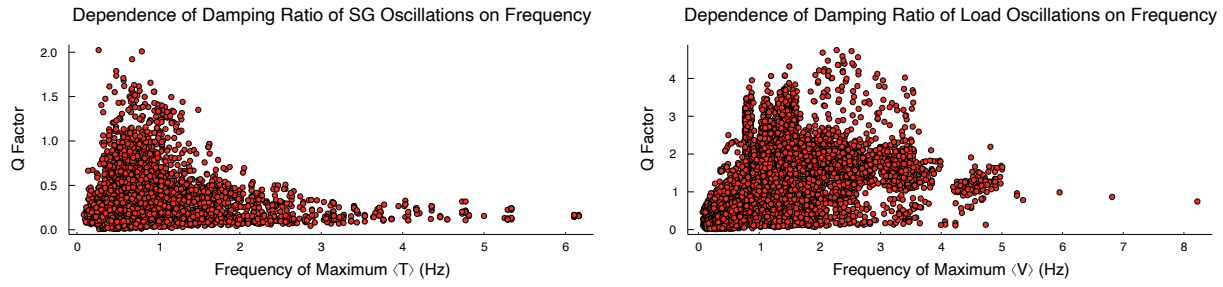


Figure 4.4: The quality factor, which is related to the damping ratio, of each peak as a function of the frequency of the peak. Each point is one peak from one scenario, and all peaks from all scenarios are plotted. The left plot shows the peaks in the kinetic energy, and the right plot shows the peaks in the nodal potential energy.

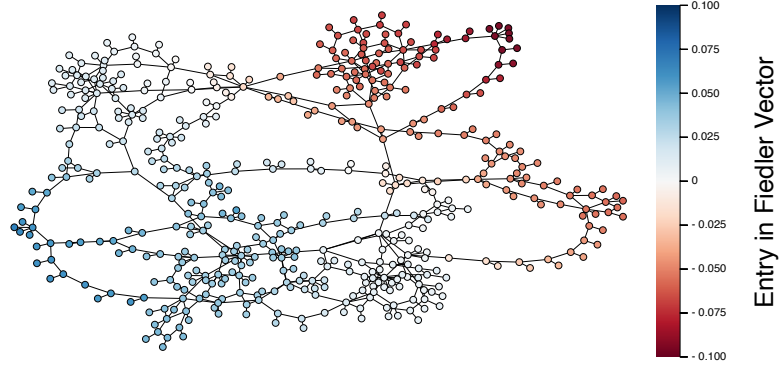


Figure 4.5: The power system test case where each node is colored by the value of its entry in the Fiedler vector.

[citation].

[I think I need a paragraph here that summarizes this section and what the main points the reader should take away.]

4.2 Identification of Inter-Area Oscillations

As mentioned earlier, the second type of oscillatory behavior studied in this work is inter-area oscillations. The most consistently used method for identification of inter-area oscillations is via the frequency of the excited network mode (see Section 2.1.3). Inter-area oscillations are typically observed to occur at a frequency range of blah-blah [citation]. This coincides with lower network modes (*i.e.* smaller eigenvalues). Rather than monitor the frequencies of the network to determine if an inter-area mode is excited, I instead pick a network mode to monitor and measure how much it participates in the oscillatory behavior. In this work, I monitor the mode associated with the second smallest eigenvalue, often called the Fiedler vector (see Section 2.1.2). It is known that the Fiedler vector bisects a graph, such that it minimizes the number of edges that connect vertices in opposite areas [citation]. Thus, two subgraphs can be defined for a network which are defined by the entries of the Fiedler vector. As an example, Figure 4.5 plots the 500 node network test case and colors each node by the value of its entry in the Fiedler vector. Notice that there is a clear separation of the red and blue nodes which correspond to the negative and positive entries in the

Fiedler vector. I define area 1 as the nodes which have a negative entry in the Fiedler vector (red), and area 2 consists of the nodes with a positive entry in the Fiedler vector (blue).

For each scenario, I quantify the response of each area via the RMS of the total oscillatory energy ($\langle T + V \rangle$) of the two subgraphs. As an example, Figure [blah] shows the RMS of the total energy for each area as a function of the VRG inertia value for one scenario. The colors of the traces indicate the two areas and they correspond to the colors in Figure 4.5. ***The VRG is located in area 2.**** At smaller inertia values, the total oscillatory energy of area 2 is significantly larger than that of area 1. This indicates that the area that contains the VRG absorbs most of the perturbations. Interestingly, a peak occurs in area 1 at a VRG inertia value of approximately 8.5, which is larger than the range of inertia values that coincide with the local plant oscillations (0.01 – 8). This suggests that the perturbation energy is no longer localized to various subgraphs of the network, but instead it has become delocalized and thus is being absorbed by many network components. Thus, the value where the peak occurs for the area that does not contain the VRG can be thought of as a transition point from local plant oscillations to inter-area oscillations.

4.3 Transition Dependence on Network Structure

The results presented above indicate that local oscillations occur at smaller inertia values (and thus larger frequencies) than inter-area oscillations. This is consistent with previous work [citations]. However, the value where this transition occurs is not the same for all network locations. Consider a VRG location that is electrically distant from other SGs and a VRG location that is electrically close to other SGs. By the definition of the natural frequency, the electrically distant VRG needs a smaller inertia value to achieve the same natural frequency as the electrically close VRG. In other words, the more electrically distant a VRG is the less inertia is required to induce inter-area oscillations.

To validate this, Figure 4.6 plots the closeness centrality of each VRG network location as a function of the inertia value where inter-area oscillations occur. The color of each point indicates the VRG's value in the Fiedler vector. In general, the larger the closeness centrality, the larger the

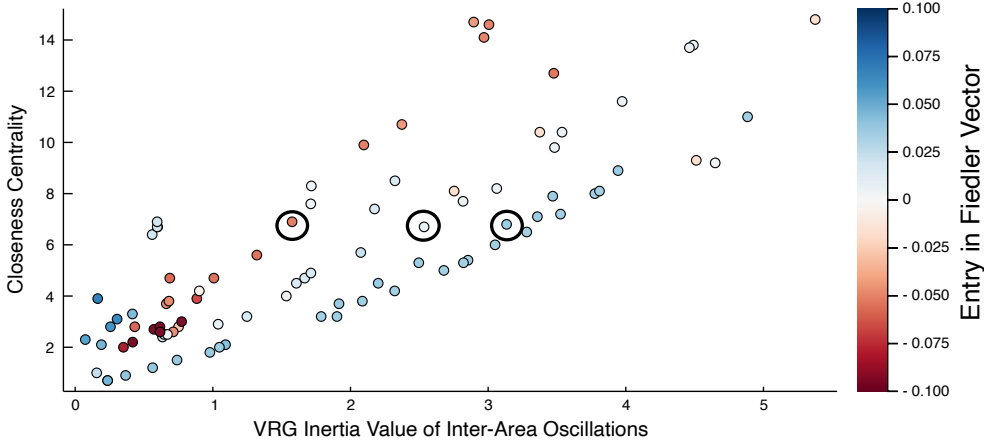


Figure 4.6: Closeness centrality of each VRG network location as a function of the VRG inertia value where inter-area oscillations occur. Each point is colored by the Fiedler entry of the VRG node.

inertia transition value. Specifically, there appears to be an almost linear relationship between the inertia transition value and the closeness centrality. The linearity is consistent with the relationship between the natural frequency, the electrical distance, and the inertia value, since the frequency where inter-area oscillations occur is approximately the same for each scenario.²

Although the linearity between electrical distance and the VRG inertia transition value is expected, there is other structure in Figure 4.6 that is not expected. There are three almost linear branches in this plot which appear to coincide with three different parts of the network: the most negative Fiedler entries (red) are the upper branch, the most positive (blue) are the lower branch, and finally the almost-zero Fiedler entries (white) make up the middle branch. The three branches are particularly distinct at larger inertia values; at smaller inertia values the branch separation is less apparent. Consider the three circled points in Figure 4.6. All three of these points have similar global network positions as indicated by the fact that the closeness centralities are approximately the same. However, the blue point has a much larger inertia transition value than the red point. This suggests that the *local* structure of the blue and red areas has a significant impact on the transition. In particular, generators in the red area must be more central than those in the blue

² because I am measuring the same mode for each scenario

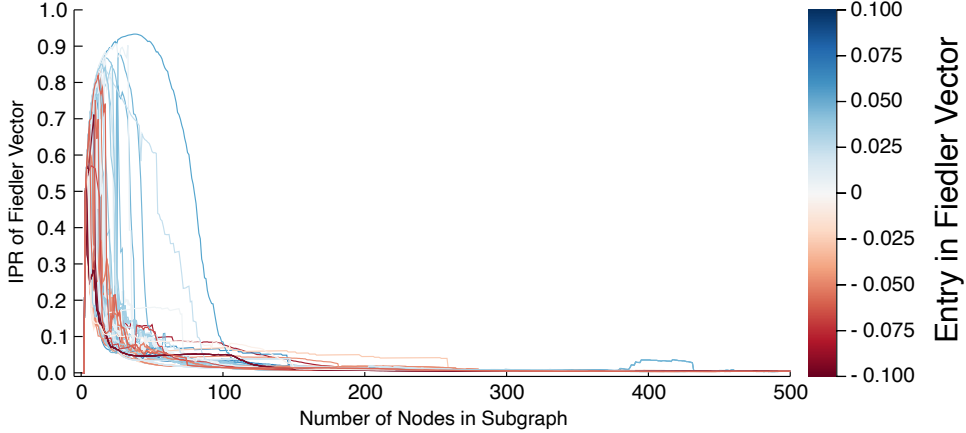


Figure 4.7: IPR of Fiedler vector as a function of the number of nodes in the subgraph.

area to achieve similar small-signal dynamics (*i.e.* the same inertia transition value). Although the global network location, as quantified by the closeness centrality, is clearly related to the transition from local to inter-area oscillations, it does not explain the three branches in Figure 4.6. This suggests that a local measure of the network structure may better explain the dependence of the VRG inertia transition value on the VRG network location.

To explore this idea further, I quantify the local network structure of a VRG location by measuring the inverse participation ratio (IPR) of the Fiedler vector of various subgraphs. Recall from Section 2.1.2.1 that the IPR of the k th eigenvector v^k is defined as $\text{IPR}_k = \sum_{i=1}^N (v_i^k)^4$. When $\text{IPR}_k = 1$ this indicates that the eigenvector entries are all zero except for one (*i.e.* the eigenvector is completely localized). For each VRG location, I measure the IPR of the Fiedler vector (call this IPR_2) for a sequence of subgraphs. The subgraphs are constructed from the local neighborhood of each VRG location. Let S_i^g represent the subgraph that includes the i closest nodes to the VRG g . I measure IPR_2 for the sequence of subgraphs $\{S_g^2, S_g^3, \dots, S_g^{n-1}, S_g^n\}$.

Figure 4.7 plots IPR_2 of the subgraph sequence for each VRG location as a function of the number of nodes in the subgraph. The color of each line indicates the VRG's entry in the Fiedler vector. Every line begins and ends at the same value (approximately 0.1) because the first and last subgraphs are the same for each VRG location. Each trace in Figure 4.7 has a peak within the

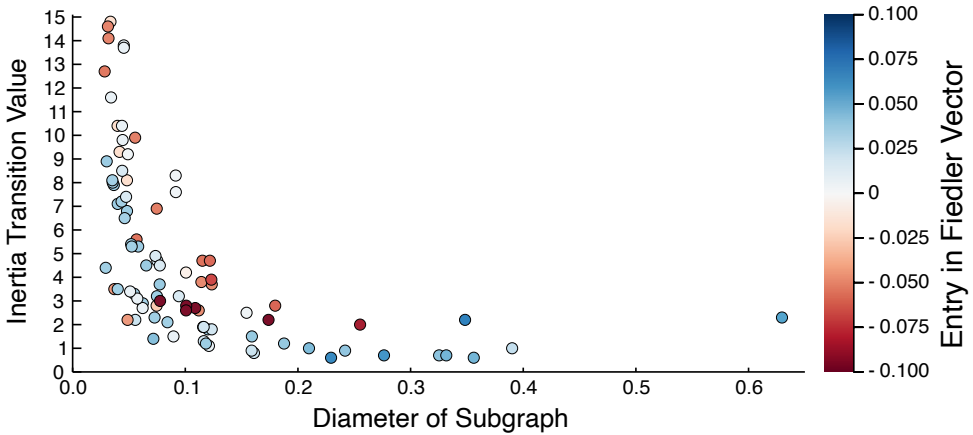


Figure 4.8: Dependence of inertia transition value on the diameter of the local subgraph with the most localized Fiedler vector.

first 100 node additions, and the IPR is clearly very sensitive in this regime. The peaks in the IPR indicate the VRG neighborhood subgraphs with the most localized Fiedler vector.

[More explanation needs to come here to explain why I did this next step.]

Figure 4.8 plots the VRG inertia transition value as a function of the diameter of the subgraph associated with the peak IPR_2 . There is a clear non-linear relationship between the transition value and the size of the local subgraph. Specifically, as the diameter of the subgraph decreases (*i.e.* the nodes are closer together) the inertia transition value increases. This means that the closer together the nodes of in the neighborhood surrounding the VRG are, the more inertial support that VRG location can provide.

This indicates that the VRG inertia transition value is dependent on the local network structure of the VRG location.